Preprint -- accepted for publication May 2010

ROCR: An Energy-Efficient Dynamic Wall-Climbing Robot

William R. Provancher*, *Member, IEEE,* Samuel I. Jensen-Segal, and Mark A. Fehlberg

***Abstract*—We present a novel bioinspired dynamic climbing robot, with a recursive name: ROCR is an Oscillating Climbing Robot. ROCR, pronounced "Rocker," is a pendular, two-link, serial-chain robot that utilizes alternating hand-holds and an actuated tail to propel itself upward in a climbing style based on observation of human climbers and brachiating gibbons. ROCR's bioinspired pendular climbing strategy is simple and efficient. In fact, to our knowledge ROCR is also the first climbing robot that is designed for efficiency. ROCR is a lightweight, flexible, self-contained robot. This robot is intended for autonomous surveillance and inspection on sheer vertical surfaces. Potential locomotion gait strategies were investigated in simulation using Working Model 2D, and were evaluated on a basis of climbing rate, energy efficiency, and whether stable open-loop climbing was achieved. We identified that the most effective climbing resulted from sinusoidal tail motions. The addition of a body stabilizer reduced the robot's out-of-plane motion at higher frequencies and promoted more reliable gripper attachment. Experimental measurements of the robot showed climbing efficiencies of over 20% and a specific resistance of 5.0, while consuming 27 J/m at a maximum climbing speed of 15.7 cm/s (0.34 body lengths/s) – setting a first benchmark for efficiency of climbing robots. Future work will include further design optimization, integration of more complex gripping mechanisms, and investigating more complex control strategies.**

***Index Terms*—Climbing robot, bioinspired design, efficiency, dynamics.**

I. Introduction and Background

Robots can be designed to work in hostile [1], dangerous [2], or challenging environments [3]. Most climbing robots are intended for maintenance or inspection in environments such as the exteriors of buildings, bridges or dams [4], [5], [6], [7], [8], [9], storage tanks [10], [11], [12], nuclear facilities [2], or reconnaissance within buildings [13], [5].

Climbing robots face a variety of challenges distinct from those faced by ground-traversing robots. Such challenges include needing to fully lift their entire mass in order to make vertical progress as in the case of "pull-up" style climbers, physically holding onto a vertical surface, maneuvering laterally or over surface features, and self-orienting in the vertical plane. In recent years, climbing robots have become lighter, more adaptable to a wide variety of surfaces, and much more sophisticated in their functional capabilities. These advances have been driven by improved manufacturing techniques, increased microcontroller computational power, and novel strategies for climbing.

Haptics and Embedded Mechatronics Lab, University of Utah, Salt Lake City, Utah. *For correspondence, contact wil@mech.utah.edu.

Manuscript submitted 12/18/2009; revised 4/18/2010; accepted 5/28/2010.

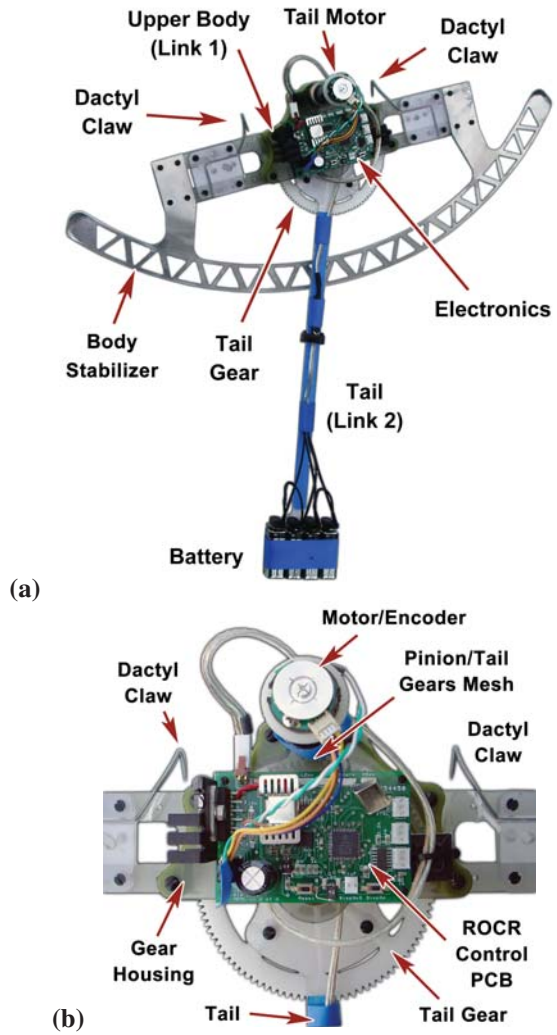

Fig. 1. (a) Second-generation prototype of ROCR, with geared DC motor, dactyl claw gripping mechanisms, and electronics including microcontroller (MCU), accelerometer, and H-bridge. The robot is powered by its tail-mounted battery. (b) Detailed view of ROCR's upper body showing external motor pinion gear and tail gear, adjustable dactyl claws, and circuit board (PCB).

Many climbing robots are large and are intended for maintenance and inspection purposes. Two to eight legs are predominant, although some researchers have investigated vacuum-based hovercraft-type robots that drive on the walls [4], [14]. Typically, more than two legs provide redundant support and often increase load capacity and safety. However, these benefits are achieved at the cost of increased complexity, size, and weight. Legged robots offer greater adaptability to variations in the climbing surface, but they require greater

intelligence to control their foot placement and interaction with the wall. In contrast, the wall-driving robots move over small asperities easily, but any appreciable surface variations disrupt their vacuum and may cause them to fall.

For applications such as surveillance or inspection, small robots are often preferred [5], [11]. Due to size constraints, feet are proportionally smaller and resulting capacity limitations require these robots to be very lightweight. Depending upon the surface, such feet typically use suction cups [15], [16], [17], [18], [2], [19] or vacuum-adhesion systems [20], [21] for clean nonporous surfaces, magnetism for ferrous surfaces [22], [23], [24], [25], [26], [27], [28], or grippers for gussets and protrusions [29]. Elastomer and pressure sensitive adhesive-based grippers [30], [31], [32] provide good adhesion to clean surfaces. Researchers have also long pursued gecko-inspired dry-adhesive grippers [33], [34], [35], [36], [37] for truly multipurpose gripping, with significant progress in recent years [37], [36]. Electrostatic adhesion, recently demonstrated by SRI, is also quite promising [38]. Spiny grippers have been successful in providing reliable griping on rough surfaces [39]. Several such wall climbing robots also utilize inward pulling motions with their feet to improve attachment, as inspired by cockroaches and geckos [39], [40], [41], [42]. Also taking a cue from biology, Koditschek's group has developed a robot called DynoClimber that pulls and swings its way up a wall and is tuned to match the reaction forces observed in geckos [43]. More recently, this robot has been tuned to achieve high-speed vertical climbing [44]. DynoClimber bears some similarity to the authors' climber ROCR; however, ROCR's design utilizes a single revolute actuator rather than multiple crank-slider mechanisms to provide locomotion (see Fig. 1).

Climbing robots employ many types of mechanical actuation devices to facilitate their climbing strategies, including wheels [33], tracks [38], [45], actuated arms [25], [46], pneumatically actuated systems [2], and cables [24]. Many of these climbing strategies have been inspired by observation of the natural world. The core innovations of ROCR – its energy-efficient climbing strategy and simple mechanical design – arise from observing mass shifting in human climbers and brachiative motion in animals. The resultant, body-oscillating, mass-shifting climbing strategy is energy efficient and enables a wide range of climbing gaits to suit different surfaces, tasks, and power or weight requirements. While pendular mass shifting has been previously explored as a means of dynamic wall climbing [43], [44], ROCR focuses on the benefits this climbing strategy offers in terms of energy efficiency and mechanical simplicity.

Proficient human climbers take advantage of both subtle and dramatic mass shifting to gain elevation while minimizing energy expended. A simple lateral body movement prior to changing handholds often enables a human climber to reach higher with less pull-up effort. Human climbers often engage in dramatic mass shifting in preparation for highly dynamic climbing motions, essentially winding-up and then releasing their potential energy (PE) into a large vertical gain. Stringing such motions together is also used by primates to brachiate in arboreal environments. Brachiation is most notably employed by gibbons when they swing from one handhold to the next in a very dynamic pattern of gripping and swinging [47]. Brachiative motion strings together a sequence of pendular paths with coordinated grip changes to achieve lateral motion. In this method of lateral swinging motion, very little input energy is required to maintain physical progress [48], [49]. ROCR turns standard gibbon brachiation vertical, combining it with human-style mass shifting into a tail-swinging, body-oscillating scansorial climbing strategy. As expected with a pendular system, maximum efficiency can be achieved by targeting the natural frequency of the system, as has been previously done with ground-traversing robots [50], [51].

By mimicking climbing strategies employed by human climbers and animals, a simple, energy-efficient climbing strategy has been developed. Our two-link oscillating climbing robot, ROCR, uses precise mass shifts, affected by carefully controlled tail motions to raise one hand/gripper at a time. Combining and integrating these behaviors enables ROCR to climb efficiently with a minimum of moving parts. In this paper we provide details of ROCR's design, including its dactyl claw grippers and on-board electronics. We explain ROCR's locomotion strategy and present our dynamic model and simulation results. We then describe experiments that were conducted to assess the efficiency and climbing speed of our prototype that were enabled with the addition of a body stabilizer.

II. Robot Design

A. Mechanical Design

ROCR is a pendular, two-link, serial-chain robot with a pivoting tail attached to the center of its first link (see Fig. 1). It has two dactyl claw gripping mechanisms whose location may be adjusted along the width of the upper body (link 1). The grippers are made from 1.0 mm diameter spring steel that is bent such that they provide directional adhesion. That is, ROCR's claws bear weight when pulled downward, but automatically release when the the force on the claw is reversed. This behavior is facilitated by the angle at which the claws are bent. As shown respectively in Figs. 1(b) and 6, the claws have their tips bent $\sim 5^\circ$ toward the robot's centerline and $\sim 45^\circ$ downward, to permit the claw's sharp tips to glide over the carpet when climbing upward.

Directional adhesion has also been utilized with several other biologically inspired gripping mechanisms, e.g., [41], [39], [37], [40], [44]. Directional adhesion allows ROCR to automatically ratchet up a wall without carefully coordinated gripping, as was required in the first generation design of ROCR that utilized magnetic grippers (see [52], [53]). The dactyl claw design was adopted to allow the authors to focus on the dynamics and efficiency of ROCR, as has been employed by prior climbing robot researchers to focus on non-adhesion related research, e.g., [41], [43].

ROCR's overall length and mass are 46 cm and 0.55 kg, respectively. The upper body (link 1) is 31.1 cm across by 4.4 cm tall, the tail is 40.6 cm long, with 36.8 cm between the tail pivot and the center of the 0.22 kg tail mass. Although the spacing of the dactyl claws is adjustable, the spacing between claws is set at 92 mm and 124 mm in the experiments

described in this paper. A body stabilizer was added to ROCR to improve gripper attachment. The body stabilizer is made from 1.5 mm thick aluminum and weighs 23 g. It rigidly attaches to the ends of ROCR's arms and is designed as a 33 cm radius arc section to better slide over the wall and is ∼49 cm wide. The body stabilizer extends downward approximately 11 cm below the tail pivot in the center of the robot. The left and right ends of the 2.5 cm wide arc section are bent and rounded in a manner similar to the tip of a ski to allow the stabilizer to slide more easily on the wall. The addition of the body stabilizer significantly improved the attachment capabilities of the robot by keeping the motion of the robot more constrained to the plane of the wall. This led to nearly a twofold increase in measured speed and efficiency over prior recorded data shown in [53].

The driving requirement for tail actuation stems from the desire to have the robot quasi-statically lift the weight of its tail mass at low tail frequencies. This was necessary in order to fully investigate the robot's climbing efficiency as a function of tail frequency. The tail actuation torque required for the robot to climb quasi-statically is nearly 0.80 N-m.

As an improvement to ROCR's first-generation direct-drive tail design (see [52]), the current design employs a more lightly geared (19:1 GP16A) 4.5 Watt RE16 motor, which drives a set of external gears. In this design, a 15 mm diameter acetal pinion gear drives a larger 100 mm diameter acetal gear that is attached to the tail at the tail pivot, resulting in a total gear ratio of 126.7:1 for the gear train (acetal gears were purchased from Stock Drive Products/Sterling Instruments). This gear ratio allows ROCR to be able to generate tail motions at up to 2 Hz. To reduce weight, the tail gear was machined to leaving only 8 radial spokes for transmitting torque and attachment to the tail. A slotted motor mount allowed for adjusting the meshing of these gears.

Use of the external pinion and tail gears has two key benefits: 1) it reduces the torque experienced at the motor's gearhead below specified limits (0.225 N-m), and more importantly, 2) it results in a back-drivable drive train that inherently limits the torques imparted to the gearhead. The torque capabilities of the robot's tail drive could be further reduced if only dynamic climbing gaits were to be attempted.

The tail is capable of swinging 78° before interference with the tail gear's housing. ROCR's RE16 tail motor uses a 100 cpr encoder to track tail position. The robot's tail position resolution is $0.014°$ per encoder tick when read in 2X quadrature mode. Note, however, that the quoted resolution neglects gear train backlash and tail compliance, which is on order of a few degrees as measured at the tail mass.

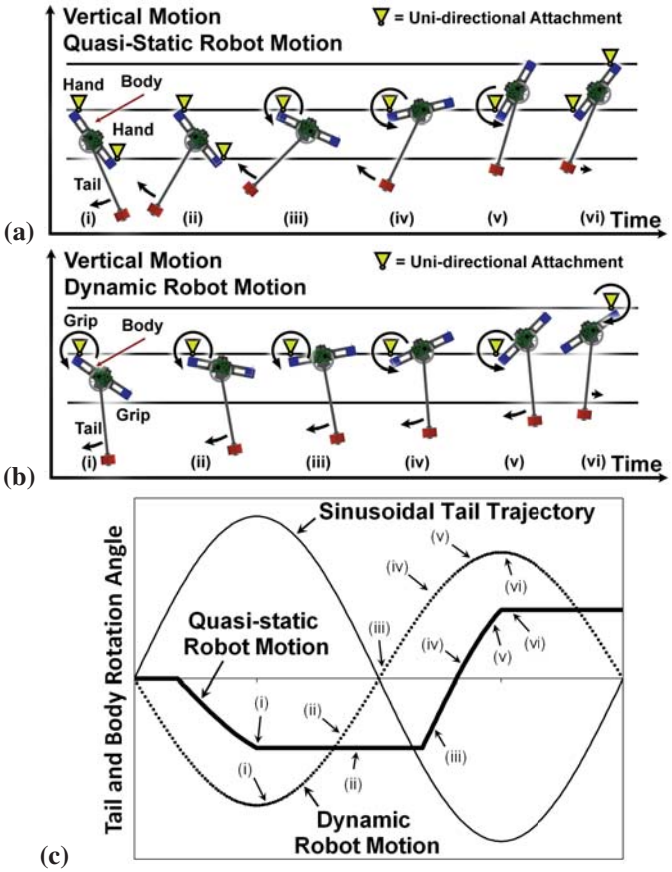

Fig. 2. Example climbing gaits for ROCR. (a) A quasi-static mass shifting, equilibrium-based gait. (b) An oscillating dynamic gait achieves higher efficiency as the system approaches resonance. Robot motions resulting from a half period of tail motion is shown in (a) and (b). An engaged uni-directional gripper is shown as a yellow triangle. Arrows indicate tail motion relative to robot body and body rotation about an engaged gripping mechanism. (c) Plot of resulting quasi-static and dynamic body motions for one period of sinusoidal tail motion. Higher frequencies result in dynamic climbing. Labels (i) through (vi) correspond to the images in (a) and (b). For (c), quasi-static robot motion (the heavier solid line) was started with the upper body horizontal as was done in our experiments, whereas the dynamic motion curve shows equilibrium steady state upper-body motion.

B. Robot Electronics

ROCR is controlled by a programmable dsPIC30F4011 microcontroller (MCU) on a custom printed circuit board (PCB) (shown in Fig. 1(b)). This PCB includes a 5 volt linear voltage regulator to supply the MCU and digital electronics, an H-bridge, a split ground plane to reduce signal interference between the H-bridge and MCU, a three-axis MEMS accelerometer, serial output, and low-profile, robust electrical headers throughout. In addition, the current electronics retain all previous design functionality from the first generation ROCR prototype [52], which utilized magnetic grippers, each with an optical encoder that was used to track robot orientation via additional XOR and comparator logic. The first-generation ROCR design also utilized RC hobby servos to actuate its grippers, and an optical range finder. The additional input and output headers used to interface these electronics were kept on the current electronics as they add negligible mass and may be utilized as needed to facilitate future climbing strategies, grip mechanisms, and climbing surfaces. In addition, the robot can also be equipped with wireless serial communication via an XBee transceiver (Digi International) PCB that has been specially designed to mate with the current ROCR electronics.

C. ROCR's Locomotion Gaits

ROCR's bioinspired oscillating climbing strategy is the key to its efficient climbing gaits. ROCR alternately grips the wall with one hand at a time and swings its tail, causing a

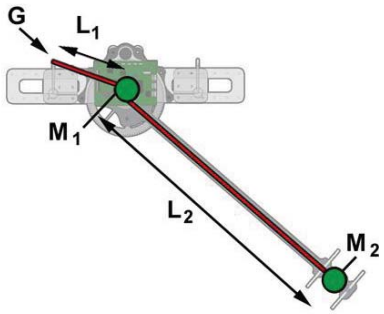

$$f_{1,2} = \frac{g^{1/2}}{2^{3/2}\pi}\left\{\left(1+\frac{M_2}{M_2}\right)\left(\frac{1}{L_1}+\frac{1}{L_2}\right) \mp \left[\left(1+\frac{M_2}{M_1}\right)^2\left(\frac{1}{L_1}+\frac{1}{L_2}\right)^2 - \frac{4}{L_1 L_2}\left(1+\frac{M_2}{M_1}\right)\right]^{1/2}\right\}^{1/2}$$

Fig. 3. Lumped-mass model of ROCR used in theoretical resonance frequency calculation. Green circles represent lumped masses M_1 and M_2. Red lines indicate massless pendular connecting rods having lengths L_1 and L_2. The double pendulum pivots at M_1 and at the grip engagement point, indicated by G.

center of gravity shift that raises its free hand, which then grips the climbing surface as portrayed in Fig. 2. The hands swap gripping duties and ROCR swings its tail in the opposite direction. As ROCR's tail oscillates from side to side, the resultant center of gravity changes, which when coordinated with gripping activity (whether gripping is active or passive), will drive the robot up a vertical surface.

As general guidance in designing ROCR and predicting its dynamic behavior, we refer to the closed form solution for a lumped mass double pendulum presented in [54]. Theoretical resonance frequencies, in Hz, are predicted by the equation shown in Fig. 3 (from [54]).

In utilizing this equation, the robot is modeled as shown in Fig. 3. For the robot design described in Section II-A, this equation predicts resonant frequencies of $f_{1,2}$ = 0.79, 2.52 Hz with link 1 of Fig. 3 with lumped mass M_1 = 0.33 kg and link length L_1 = 70.9 mm (=$\sqrt{(92\text{mm}/2)^2 + (54\text{mm})^2}$), taken as the distance between a dactyl claw and the tail pivot, and link 2 with lumped mass M_2 = 0.22 kg and link length L_2 = 368 mm, taken as the distance between the tail pivot and the tail mass' centroid (refer to Fig. 3). When the spacing between claws is 124 mm rather than 92 mm, this results in $f_{1,2}$ = 0.78, 2.36 Hz.

Although ROCR's design doesn't perfectly match this ideal lumped-mass model for a double pendulum, the predicted lower resonance frequency nearly matches a bifurcation in ROCR's climbing behavior. Two primary gaits result from varying the frequency of ROCR's sinusoidal tail motion: a quasi-static climbing gait results from tail motions below ROCR's first resonance frequency, and dynamic climbing results at frequencies above this point. These gaits result from using dactyl-claw grippers, which enforce uni-directional velocity constraints at the wall attachment.

Refer to Fig. 2 to better understand these two gaits. The quasi-static climbing, shown in Fig. 2(a), that results from slow tail frequencies can be predicted through basic statics equations, hence why we refer to it as "quasi-static." Fig. 2(c) shows the robot's motion over one period of tail motion. The tail motion is the sinusoidal curve with the lighter solid line font. The corresponding quasi-static motions of the robot's upper body are shown in the heavy solid line font with labels (i)-(vi) that correspond to the images from Fig. 2(a). The quasi-static motions in Fig. 2(c) are based on idealized equilibrium calculations, where the robot's upper body was started in a horizontal orientation, as was done in our experiments and simulation. Note that both claws bear weight during quasi-static climbing at points (i) and (ii) with more weight shifting onto the left claw as the time line progresses to frame (iii). This period of double stance is shown in the flat horizontal regions of the plot, as the tail mass has not yet shifted the robot's center of gravity to the left of the left claw. Hence, there is an apparent, pause in the robot's motion during quasi-static climbing as the tail reverses direction. Interestingly, at or near the first resonance frequency climbing ceases as the quasi-static gravitational forces are experienced for an insufficient time to allow the body to rotate against static friction. Simultaneously, the net dynamic torques about each claw is still too small for the opposite claw to rise.

As the frequency at which the tail is driven is increased, the dynamic reaction forces begin to dominate and dynamic climbing begins to result as shown in Fig. 2(b). The resulting steady state dynamic body motion, obtained through simulation, is shown by the dotted curve in Fig. 2(c). A comparison of frame (ii) in Fig. 2(a) and Fig. 2(b), shows that the upper body (link 1) has already begun to move in Fig. 2(b), frame (ii), due to the dynamic reaction forces even though the robot's center of gravity is still between its claws. For all observed dynamic climbing (experimental and simulated) between 1 and 1.5 Hz, the phasing of the tail and body motions remained $\sim$180° out of phase.

D. Software Architecture and Controls

The software development strategy for ROCR has been to build robust and flexible software, incorporating modular code wherever possible. A variety of control schemes were investigated, but a position-based tail controller using table look-up was found to be the most flexible for the open-loop climbing trajectories we adopted.

ROCR's Microchip dsPIC30F4011 microcontroller (MCU) carries out tail position control and directly reads the robot's tail position using its 16-bit Quadrature Encoder Interface (QEI) to read ROCR's RE16 tail drive motor. The tail motor encoder is run in 2X quadrature mode instead of 4X quadrature mode to keep the size of tail position variables limited to 16-bit integers.

The robot's sinusoidal tail trajectories used in the experiments reported herein are generated by table look-up. The look-up table stored 100 positions corresponding to only one quarter of a sine wave, rather than the full sine trajectory, in order to reduce the required MCU memory. Our tail controller incremented and decremented through this table to generate the first half of the sine trajectory and then negated the table values and repeated stepping through the table to complete the sinusoidal tail trajectory. The stored table values correspond to the encoder count for each desired tail position in the sine trajectory and are stored as a 100 element array of integers. This is done to avoid using computationally expensive floating point math.

A full PID controller, including integrator anti-windup, is written for ROCR, but in practice only the proportional term is required to tune the tail's position controller due to the robot's high gear ratio (126.7:1). Both the slower quasi-static and faster dynamic gaits (see Fig. 2) were successfully implemented with sinusoidal tail trajectories using a simple proportional controller on tail position. The controller output is provided to the robot's H-bridge motor amplifier as a PWM duty cycle. The tail's oscillation frequency was prescribed by varying the servo-loop interrupt from 25-1.25 ms to execute tail frequencies of 0.1-2.0 Hz. Controller performance was verified under climbing conditions with maximum steady state position error of $\sim$0.9°. Controller performance plots can be found in [53].

III. Modeling and Simulation

To evaluate the climbing strategies of ROCR and to fine tune the physical parameters of the robot, dynamic simulation was performed using Working Model 2D. Most early climbing strategies that were investigated were extremely sensitive to the specific control logic and timing. However, it was found that when a sinusoidal tail motion trajectory was combined with directionally adhesive grippers that a wide range of tail frequencies and amplitudes resulted in stable climbing. A common climbing instability that was observed in earlier gait strategies was that the robot would invert its swinging motion and begin to spin out of control. Rather than focusing on these earlier climbing strategies, we present our simulation results reflecting the current robot design and climbing strategy.

It was difficult to tune the simulation model to work well for both low-frequency and high-frequency tail motions. Furthermore, when trying to simulate lower frequency climbing with Working Model 2D, we encountered numerical chatter in the quasi-static gait when the robot was supported simultaneously by 2 claws, as seen at label (ii) in Figs. 2(a) and 2(c). The numerical chatter made it difficult to introduce robust logic for implementing the claw constraints in the simulation. To eliminate this issue, our model simply switches which *single* claw constraint is actively supporting the robot at the point when the robot's upper body (link 1) changes directions. This is a good representation of actual motion during dynamic climbing. Hence, we chose to simply focus on the high-frequency modeling, as this is the regime where desirable high-efficiency climbing occurs.

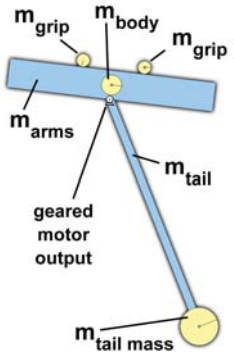

Fig. 4. Working Model 2D simulation model of ROCR. Masses shown: m_{arms} = 103 g, m_{tail} = 30 g, $m_{tailmass}$ = 220 g, m_{body} = 168 g, and m_{grip} = 15 g. m_{body} represents the combined mass of the motor, gears, and electronics.

ROCR was modeled with two rectangular solids for the upper body cross-member (m_{arms} = 103 g, 31.1 x 4.4 cm) and the tail (m_{tail} = 30 g with 36.8 cm between the tail pivot and center of the tail's end mass). The model also has four lumped masses placed at the end of the tail ($m_{tailmass}$ = 220 g), center of the body (m_{body} = 168 g), and one each at the grippers (m_{grip} = 15 g) (see Fig. 4). The "body mass" m_{body} represents the mass of the geared motor, external acetal tail gears and bearings, the external gear housing, and the robot's electronics. The spacing between claws was set at 92 mm and 124 mm for our simulations to match experimental conditions.

The model also includes a small amount of rotational damping (0.5 mN-m-s/Rad) at the claw about which the robot is actively swinging. Rotational damping at the claw pivot was a convenient way to represent the drag forces of the robot's body sliding over the wall and other parasitic forces that were present. The rotational damping added stability to the simulation and was empirically tuned such that the simulation matched the actual climbing behavior observed when climbing dynamically (1-1.5 Hz). Simulation results are presented along side our experimentally measured results for climbing speed and efficiency (see Table I). Fig. 5(a) provides typical Working Model 2D climbing simulation data showing the location of ROCR's upper body's center of mass while climbing. Its periodic motion accurately represents ROCR's actual climbing behavior, which is shown in Fig. 5(b).

To evaluate the energy efficiency of ROCR's design, the amount of energy consumed by ROCR's drive motor was calculated for each time step. The energy calculation was based on the commanded input torque to the motor. These torques were calculated by a simulated proportional motor position controller and were related to motor current by the RE16's motor constant, K_t. The power was calculated using the following ideal motor equations:

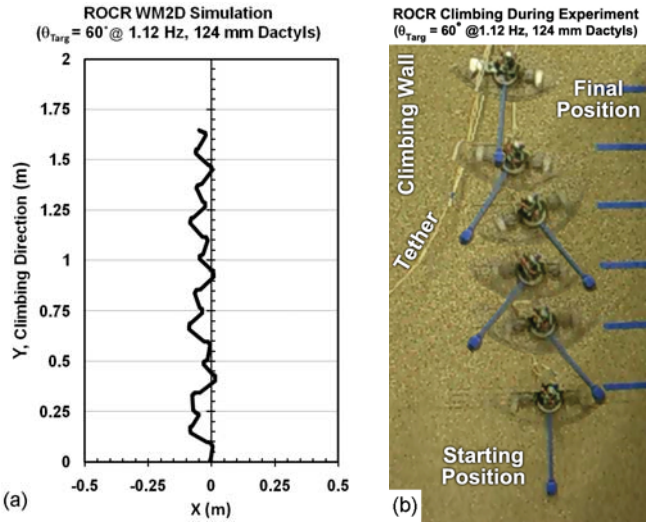

Fig. 5. ROCR simulation data from Working Model 2D and corresponding robot images from experimental testing for tail motions of θ_{Targ} = 60° at 1.125 Hz and a 124 mm dactyl claw spacing. These conditions correspond to the most efficient climbing conditions recorded experimentally, as reported in Table I. (a) The plotted simulation data represents the location of the center of mass of the upper body (link 1). Elapsed time = 8.9 seconds. (b) Image from experimental testing with ROCR. Several frames were extracted from video, cropped, and then composited together into a single image.

$$i_{motor} = \frac{\tau}{K_t G_{gearratio}} \quad (1)$$

$$v_{motor} = \omega_{tail} K_b G_{gearratio} + R_{motor} * i_{motor} \quad (2)$$

$$P = v_{motor} * i_{motor} \quad (3)$$

where i_{motor} is the motor current, τ is the torque at the tail pivot, K_t is the motor's torque constant, and $G_{gearratio}$ is the gear ratio that results from the product of the motor's gearhead and the external gearing (126.7:1). In addition, v_{motor} is the voltage applied across the motor terminals, ω_{tail} is the angular velocity of the tail, K_b is the motor's back-EMF constant, and R_{motor} is the motor's armature resistance. P is the electrical power used to drive ROCR's tail motor.

The power was then integrated in time. The total amount of locomotion energy expended by the motor is then normalized by the amount of vertical gain acquired at the end of the climbing sequence. We report the efficiency of climbing as the gained potential energy due to climbing divided by the energy consumed by the robot while climbing. Although the above idealized motor equations do not account for issues such as specific motor and gear efficiencies, they have been sufficient to predict general trends for climbing speed and efficiency, and meet the needs of our research.

IV. Climbing Experiments

ROCR was experimentally evaluated using a vertical carpeted climbing wall. Climbing rate and efficiency were computed from data taken while ROCR was run with sinusoidal tail trajectories under a wide range of tail amplitudes and frequencies. These results are tabulated and briefly compared with simulation results that were conducted under like conditions. We next outline our test procedures before presenting results.

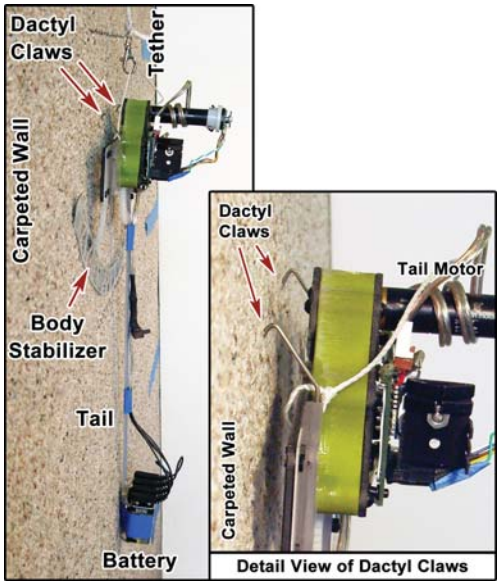

Fig. 6. Side view and detail of ROCR and its dactyl claws engaging the carpeted climbing wall.

A. Test Details

Experiments with ROCR were run on a testing surface comprised of a 1.22 m x 2.44 m sheet of 1.9 cm thick plywood covered with short nap carpet and secured to a wall such that it provides a vertical climbing surface as shown in Fig. 6. Three climbing runs, each consisting of 10 full swing periods, were performed for each tail frequency and target tail angle combination for which ROCR can reliably climb. Tail angles of $\pm 45°$, $\pm 60°$, and $\pm 75°$, were tested experimentally, where zero degrees was with the tail pointing straight downward to form a "T-shape" with the upper body. $\pm 45°$ was the smallest amplitude at which any climbing occurred for low frequencies, and $\pm 75°$ was nearly the maximum allowable angle before the tail interfered with the gear housing. Note that at the higher frequencies, $\pm 75°$ was not tested since it caused erratic climbing and unreliable attachment of the claws due to excited out-of-plane dynamic modes. The tail motion frequencies at which ROCR was tested spanned 0.33 Hz up to 1.5 Hz. Above 1.5 Hz ROCR also experienced unreliable attachment of the claws due to out-of-plane motions of the robot as previously described. The spacing between claws was set at 92 mm and 124 mm in our presented experiments.

The 92 mm claw spacing was the lower bound of claw spacing for our prototype as mounting for the claws were done with pre-drilled holes in the upper body. Moving the claws out to the next set of pre-drilled mounting holes placed the claws 124 mm apart; however, quasi-static climbing was barely possible at this spacing using the 220 g tail mass. Claw spacings wider than 124 mm produced dynamic climbing with higher amplitudes, but resulted in unreliable wall gripping; hence claw spacings wider than 124 mm were not tested.

In these experiments, ROCR is powered by a 12 V DC power supply using a tether. This was done so we could externally measure the power consumption while climbing. Comparisons of climbing with and without the tether showed

no difference in the robot's dynamics or measured climbing distance. Tail position and current data are captured for each test run. Current usage data is collected for each run at 250 Hz, using custom-built current-measurement equipment and PC-based serial data acquisition. Current data were also examined using a 20 MHz oscilloscope to confirm that a 250 Hz sample frequency accurately captured the current data. Details of the current measurement equipment may be found in [53].

B. Experimental Results and Discussion

The robot's climbing rate, energy consumed per distance climbed, and climbing efficiency are reported in Table I. Experimental results are also presented graphically in Fig. 7. A robot mass of 0.55 kg was used to compute the robot's potential energy and in turn was used to calculate the robot's climbing efficiency. Fig. 5(b) shows several images of ROCR as it climbs the wall during an actual experiment (with θ_{Targ} = 60° at 1.125 Hz and a 124 mm dactyl claw spacing). Several frames from video of ROCR climbing were extracted, cropped, and composited together to create Fig. 5(b). As can be observed from Table I, the climbing rates and efficiencies increase dramatically above 1 Hz and are reported as a maximum of 15.67 cm/s (0.34 body lengths/s) and 20.1%, respectively (this condition shown in Fig. 5(b)). This marks a nearly 500% increase over quasi-static climbing at lower frequencies. Note that, in general, climbing efficiency directly correlates with climbing rate since the power required to actively run the robot plateaus above 1 Hz, while the robot climbs ever faster with increasing frequency (see Fig. 8).

It can also be observed from both Table I and Fig. 7 that with the 92 mm claw spacing the robot is effectively *stalled* at 0.75 Hz. This is because the dynamic reaction forces have not yet become significant enough to transition from quasi-static to dynamic climbing and the peak gravitation torques are only experienced briefly and do not allow the robot's body sufficient time to pivot while overcoming coulomb friction from sliding over the wall. This behavior also occurred at the 124 mm claw spacing at 1 Hz with ±45° tail motions.

Above 1 Hz, the robot swings more freely and hence its climbing behavior is no longer dominated by static coulomb friction, as is the case for lower frequencies. The predicted and measured energy consumption is also quite close above 1 Hz, with the exception of the case for 1 Hz with ±45° tail amplitude for the 124 mm claw spacing. The robot did not climb well under these conditions due to insufficient rotational momentum provided by the small tail amplitude.

It can also be observed that the simulations generally over-estimate the climbing speed (see Table I). This is likely due to many unmodeled factors such as varying friction conditions and the loss of climbing progress each time the hooks reengage the carpet (claw engagement requires ∼5 mm of motion to sink claws into carpet). Furthermore, the simulation always switches claws at the peak reach amplitude, which is not always the case for the actual robot. Issues with claw engagement result from out-of-plane modes of motion of the robot that are strongly excited at frequencies above 1.5 Hz. These excited out-of-plane motions and chaotic behavior which become present as we approach the 2^{nd} resonance point are the primary reasons why ROCR has not climbed reliably at higher frequencies. Also consider that the reported climbing rates were taken as the average over 10 periods of tail motion with ROCR starting from a resting state; hence the final velocity is actually higher than reported in Table I. Note, however, that this does not affect our comparison of simulation and experimental data though as both were run for 10 cycles with the same initial conditions.

92 mm Dactyl Claw Spacing Data

f_{tail} (Hz)	Θ_{Targ} (deg)	Model Rate (cm/s)	Actual Rate (cm/s)	Model Energy (J/cm)	Actual Energy (J/cm)	Actual Efficiency (%)
0.33	±45°	N/A	0.52	N/A	3.88	1.34
	±60°	N/A	1.94	N/A	1.41	3.68
	±75°	N/A	3.07	N/A	1.14	4.55
0.50	±45°	N/A	0.15	N/A	17.7	0.29
	±60°	N/A	0.94	N/A	3.04	1.70
	±75°	N/A	2.16	N/A	1.25	4.15
0.75	±45°	N/A	0.19	N/A	15.7	0.33
	±60°	N/A	0.23	N/A	13.2	0.39
	±75°	N/A	0.41	N/A	6.80	0.76
1.0	±45°	11.3	4.1	0.39	0.94	5.77
	±60°	14.7	9.8	0.42	0.43	12.6
	±75°	16.4	12.8 *	0.45	0.32	17.0 *
1.125	±45°	12.7	9.1	0.39	0.48	11.3
	±60°	16.8	12.6	0.43	0.35	15.3
1.25	±45°	14.6	10.8	0.40	0.40	13.4
	±60°	16.9	11.5	0.42	0.37	14.7
1.375	±45°	16.6	10.8	0.40	0.40	13.7
1.5	±45°	16.6	12.0	0.40	0.35	15.2
124 mm Dactyl Claw Spacing Data						
1.0	±45°	14.7	1.10	0.30	12.1	0.35
	±60°	20.0	12.6	0.32	0.33	16.3
1.125	±45°	17.4	11.3	0.31	0.38	14.4
	±60°	19.7	15.7 *	0.32	0.27	20.1 *
1.25	±45°	19.3	14.0	0.31	0.32	17.1
1.375	±45°	18.7	15.1	0.30	0.28	19.1

TABLE I
EXPERIMENTAL DATA FOR ROCR WITH 92 MM AND 124 MM CLAW SPACING. RATE IS THE SPEED OF VERTICAL CLIMBING PROGRESS IN CM/S. ENERGY IS THE ENERGY USED PER CM OF CLIMBING. EFFICIENCY IS THE RATIO OF POTENTIAL ENERGY GAINED WHEN CLIMBING DIVIDED BY THE ENERGY CONSUMED. * DENOTES THE CASES FOR MAXIMUM SPEED AND EFFICIENCY FOR EACH CLAW SPACING.

Efficiency Considerations

When we refer to efficiency of our robot, it is really the *climbing efficiency* that we are referring to, which is both a function of actuator efficiency (and associated electronics) *and* coupling the motions of the actuators into climbing motion. While the coupling of the robot's motions into climbing motion is mostly a function of exciting the dynamics of the robot, creating these motions can be done in a variety of ways. So, we now take a look at the contributions to the consumed electrical power, and will then compare the efficiency of our robot to efficiency measures previously used with legged robots.

To put ROCR's currently measured 20% efficiency in perspective, it is useful to compare this to the specified peak efficiency of the Maxon RE16 motor+gearhead of 63.8% (at 48 mN-m of torque for the 19:1 gear ratio). This is derived from a peak motor efficiency of 78% and peak gearhead efficiency of 81%. This efficiency is further reduced by an

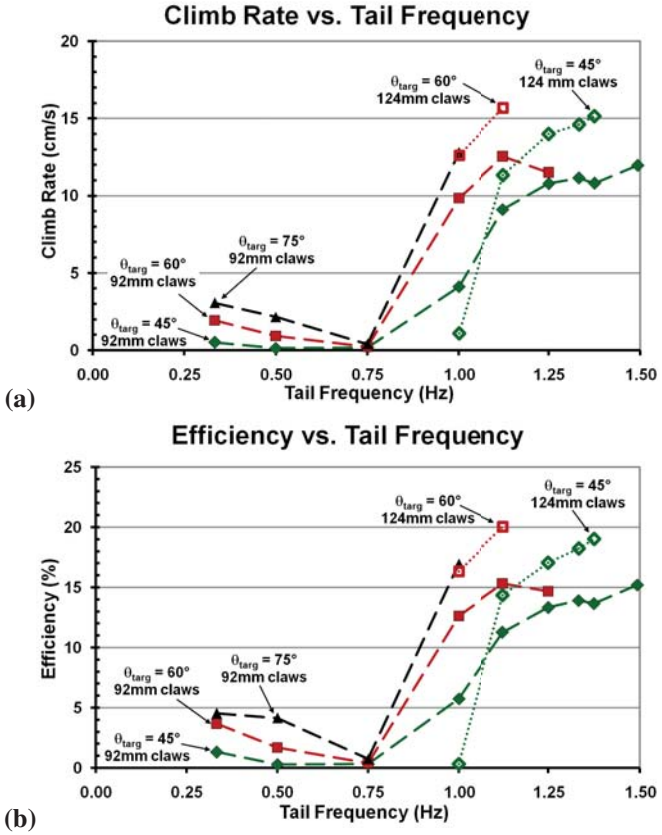

Fig. 7. Experimental results for (a) climbing rate and (b) efficiency.

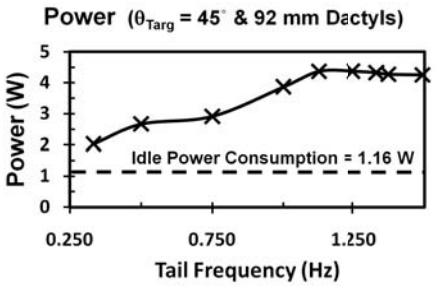

Fig. 8. ROCR's experimentally measured power while climbing. The data are for tail motions of $\theta_{Targ} = 45^\circ$ and a 92 mm dactyl claw spacing.

estimated 95% efficiency for the external acetal tail gears giving a maximum gear train efficiency of 60.6%. Hence, experimental results for the robot show approximately $\frac{1}{3}$ the maximum possible efficiency of when the motor was run under its peak conditions. It is, of course, not possible for ROCR to achieve the motor's maximum efficiency, since the motion of the tail is necessarily sinusoidal in order to achieve stable climbing motions, and the loads vary as a function of the robot's motion and orientation with respect to gravity. Using the published motor curves and efficiency data for our Maxon RE16, for the range of 1.0-1.5 Hz we estimate the average efficiency over one period of tail motion to be approximately 49-53%.

As can be observed from looking at the graph of power usage during climbing in Fig. 8, the parasitic power of the robot's electronics accounts for 1.16 W. Thus, for the measurements reported in Fig. 8, the parasitic power of the robot's electronics accounts for 27% (at 1.5 Hz) up to 57% (at 0.33 Hz) of the total power used by the robot. Under our peak operating conditions (dactyls spaced 124 mm apart, with $\theta_{Targ} = 60^\circ$ at 1.125 Hz), the electronics also account for 27% of total power draw.

Ideally we would like to compare our robot's efficiency to benchmark data, but data on power usage in climbing robots is difficult to find. Climbing roboticists tend to lionize the climbing speed, adaptability, and energy efficiency of geckos. For reference, speed data comparing ROCR's speed to other robots is provided in Table II. The type of grip mechanism used by each robot is indicated. Gecko data is included for comparison to nature's own super-climber. These remarkable animal climbers are reported to achieve 83-89% efficient climbing [55]. Direct comparisons to electrically powered climbing robots are difficult since geckos must generate their own energy biologically. Although we could not find efficiency data for any climbing robots, we did find a number of studies with legged robots that utilized *specific resistance* as a measure of efficiency.

$$Specific\ Resistance = \frac{P}{mgv} \tag{4}$$

where P is the consumed (electrical) power, m is the robot mass, g is gravity, and v is the rate of travel. For reference, a human runner has a specific resistance of ∼0.2-0.3 and the specific resistance of a gravity walker is ∼0.01-0.04.

While the legged robots that we will compare ROCR to only traverse horizontally rather than climbing, their numbers still provide a basis of comparison to ours. We can also compare ROCR with them on the basis of energy per distance traveled. Gregorio et al. optimized the design of a monopod hopper to achieve a specific resistance of 0.7 and requiring 104.2 Joules per meter traveled, when operated at a speed 1.2 m/s [56]. This specific resistance marked an order of magnitude improvement over prior hoppers. Weingarten et al. report a peak specific resistance of 0.6 for operating RHex with an optimally tuned running gait, and requiring 44 Joules per meter traveled (less optimal hand-tuned gaits for RHex had a specific resistance of 2-4) [51].

While one might expect ROCR's specific resistance to be dramatically higher than these ground traversing legged robots, it is not. ROCR's specific resistance for $\theta_{Targ} = 60^\circ$ at 1.125 Hz and a 124 mm claw spacing is 5.0, which is comparable to RHex's specific resistance when operated under the best hand-tuned conditions. ROCR also only requires 27 Joules per vertical meter of climb. So, despite the fact that ROCR is gaining potential energy as it climbs (in contrast to the above legged robots) it interestingly requires less energy per distance traveled and has a comparable specific resistance to its legged cousins. So, while it is clear that the design of ROCR can be further improved upon, its design is already competitive with highly tuned legged robots.

V. Conclusions and Future Work

We have presented the novel climbing robot, ROCR. ROCR combines mass shifting observed in human climbers with a

Author /Robot Name	Grip Mechanism	Climb Rate (cm/s)	BL/s
CMWhegs [30]	adhesive tape	5.8	0.65
Spinybot [39]	microspines	2.3	0.04
Stickybot [37]	dry adhesives	4.0	0.12
Prahlad et al. [38]	electroadhesion	15.0	∼0.4
Lynch et al. [44]	dactyl claws	66.0	1.5
RiSE [42]	dactyl claws	30.0	1.2
ROCR	dactyl claws	15.7	0.34
Gecko [41]	claws and dry adhesives	40.0	∼10

TABLE II
GRIP MECHANISM AND CLIMBING RATES (CM/S AND BODY-LENGTHS/S, INDICATED AS BL/S) ARE SHOWN FOR A NUMBER OF CONTEMPORARY CLIMBING ROBOTS AND FOR GECKOS. ROBOTS ARE LISTED BY THEIR NAME OR THE AUTHOR'S NAME.

reoriented brachiative motion observed in swinging gibbons. We report the design of the second generation robot that is autonomous and self-contained, and uses dactyl claws to adhere to a carpeted climbing wall. This prototype was built with an emphasis on mechanical simplicity, weight and energy efficiency, modularity, the ability to switch between multiple gait strategies, and autonomy. We present simulation and experimental results that show ROCR to climb with efficiencies of just over 20% – made possible by the addition of a body stabilizer to better constrain the robots motions into the plane of the wall. Furthermore, on the basis of its specific resistance, ROCR's efficiency is found to be comparable to that of highly tuned ground traversing legged robots and requiring less energy per distance traveled, despite ROCR's burden of climbing.

There are several areas for future work with ROCR, including further design optimization, integration of more complex gripping mechanisms, and investigating more complex control strategies. Further improvements in efficiency could also be made by revising the electronics.

To make the robot more versatile it would be advantageous to develop additional grippers that are compatible with the robot's locomotion strategy. Improvement of the robot's original magnetic grippers would allow it to be used on ferrous surfaces. A variety of bioinspired gripping mechanisms (e.g., similar to [39]) could also be developed to enable climbing a range of rough surface (e.g., sandstone and brick).

We are also interested in adapting the design of ROCR for use in teaching dynamics, controls, or even mechanisms design for undergraduate courses.

ACKNOWLEDGMENTS

This research was funded, in part, by the National Science Foundation under award DGE-0654414. We also wish to acknowledge help from Tom Slowik, Mike Knutson, and Keith Findling with prototyping and Steve Virost with modeling.

REFERENCES

[1] C. von Alt, B. Allen, T. Austin, N. Forrester, R. Goldsborough, M. Purcell, and R. Stokey, "Hunting for mines with remus, a high performance, affordable, free swimming underwater robot," in *OCEANS, 2001*, vol. 1, 2001, pp. 117–122.

[2] L. Briones, P. Bustamante, and M. A. Serna, "Wall-climbing robot for inspection in nuclear power plants," in *Robotics and Automation. Proceedings, IEEE International Conference on*, vol. 2, 1994, pp. 1409–1414.

[3] F. W. Bach, H. Haferkamp, J. Lindemaier, and M. Rachkov, "Underwater climbing robot for contact arc metal drilling and cutting," in *Industrial Electronics, Control, and Instrumentation., Proceedings of the IEEE IECON 22nd International Conference on*, vol. 3, 1996, pp. 1560–1565.

[4] A. Nishi, "Development of wall-climbing robots," *Computers & Electrical Engineering*, vol. 22, no. 2, pp. 123–149, 1996.

[5] M. Minor and R. Mukherjee, "Under-Actuated Kinematic Structures for Miniature Climbing Robots," *Transactions-American Society of Mechanical Engineers Journal of Mechanical Design*, vol. 125, no. 2, pp. 281–291, 2003.

[6] C. Balaguer, A. Gimenez, and M. Abderrahim, "Roma robots for inspection of steel based infrastructures," *Industrial Robot*, vol. 29, no. 3, pp. 246–51, 2002.

[7] C. Hillenbrand, D. Schmidt, and K. Berns, "Cromsci: development of a climbing robot with negative pressure adhesion for inspections," *Industrial Robot*, vol. 35, no. 3, pp. 228 – 37, 2008.

[8] R. Kamei, K. Ogasawara, and R. Katamura, "Development of multi-purpose mobile robot capable of traveling along columns and beams," in *Automation and Robotics in Construction XI. Proceedings of the 11th International Symposium on Automation and Robotics in Construction (ISARC)*, Amsterdam, Netherlands, 1994, pp. 487 – 93.

[9] B. Esser, J. Miller, D. Huston, and P. Bourn, "Robotic systems for homeland security," in *Proceedings of SPIE - The International Society for Optical Engineering*, vol. 5395, 2004, pp. 134 – 142.

[10] S. Hirose and H. Tsutsumitake, "Disk Rover: A Wall-Climbing Robot Using Permanent Magnet Disks," in *Proceedings of the 1992 IEEE International Conference on Intelligent Robots and Systems Raleigh, NC*, 1992, pp. 2074–2079.

[11] K. Kotay and D. Rus, "The Inchworm Robot: A Multi-Functional System," *Autonomous Robots*, vol. 8, no. 1, pp. 53–69, 2000.

[12] D. Longo and G. Muscato, "SCID-a non-actuated robot for walls exploration," in *Advanced Intelligent Mechatronics. Proceedings of IEEE/ASME International Conference on*, vol. 2, 2001.

[13] M. Nunobiki, M. Hasegawa, K. Okuda, N. Huruse, and Y. Takita, "Study on the gaits of an inchworm robot through a narrow path," *Advanced Robotics*, vol. 13, no. 6-8, pp. 329–330, 1999.

[14] J. Xiao, W. Morris, N. Chakravarthy, and A. Calle, "City Climber: a new generation of mobile robot with wall-climbing capability," in *Proceedings of SPIE*, vol. 6230. SPIE, 2006, p. 62301D.

[15] G. La Rosa, M. Messina, G. Muscato, and R. Sinatra, "A low-cost lightweight climbing robot for the inspection of vertical surfaces," *Mechatronics*, vol. 12, no. 1, pp. 71–96, 2002.

[16] R. Tummala, R. Mukherjee, N. Xi, D. Aslam, H. Dulimarta, J. Xiao, M. Minor, and G. Dangi, "Climbing the walls," *IEEE robotics & automation magazine*, vol. 9, no. 4, pp. 10–19, 2002.

[17] J. Zhu, D. Sun, and S. Tso, "Development of a Tracked Climbing Robot," *Journal of Intelligent and Robotic Systems*, vol. 35, no. 4, pp. 427–443, 2002.

[18] T. Yano, S. Numao, and Y. Kitamura, "Development of a self-contained wall climbing robot with scanningtype suction cups," in *Intelligent Robots and Systems. Proceedings of IEEE/RSJ International Conference on*, vol. 1, 1998.

[19] G. Dangi, J. Stam, and D. Aslam, "Design, Fabrication and Testing of a Smart Robotic Foot for Microrobotic Systems," in *International Symposium on Robotics*, vol. 31, 2000, pp. 283–287.

[20] D. Murph, "Vortex's wall climbing robot peeks in windows," *http://www.engadget.com/2007/06/29/vortexs-wall-climbing-robot-peeks-in-windows/*, 2007.

[21] S. Wu, M. Li, S. Xiao, and Y. Li, "A wireless distributed wall climbing robotic system for reconnaissance purpose," in *Mechatronics and Automation, Proceedings of the IEEE International Conference on*, 2006, pp. 1308–1312.

[22] B. Shores and M. Minor, "Design, kinematic analysis, and quasi-steady control of a morphic rolling disk biped climbing robot," in *Robotics and Automation. Proc. of the IEEE International Conference on*, 2005, pp. 2721–2726.

[23] S. Hirose, M. Imazato, Y. Kudo, and Y. Umetani, "Internally-balanced magnet unit," *Advanced robotics*, vol. 1, no. 3, pp. 225–242, 1986.

[24] M. Suzuki, S. Kitai, and S. Hirose, "Basic systematic experiments and new type child unit of anchor climber: Swarm type wall climbing robot system," pp. 3034–3039, May 19-23 2008.

[25] C. Balaguer, A. Gimnez, J. Pastor, V. Padrn, and M. Abderrahim, "A climbing autonomous robot for inspection applications in 3d complex environments." in *Robotica*, vol. 18, 2000, pp. 287–297.
[26] Y. Zhao, Z. Fu, Q. Cao, and Y. Wang, "Development and applications of wall-climbing robots with a single suction cup," *Robotica*, vol. 22, no. 6, pp. 643–648, 2004.
[27] W. Shen, J. Gu, and Y. Shen, "Permanent magnetic system design for the wall-climbing robot," *Applied Bionics and Biomechanics*, vol. 3, no. 3, pp. 151–159, 2006.
[28] J. Berengueres, S. Saito, and K. Tadakuma, "Structural properties of a scaled gecko foot-hair," *Bioinpiration and Biomimetics*, vol. 2, no. 1, p. 1, 2007.
[29] C. Balaguer, A. Gimenez, and A. Jardon, "Climbing Robots Mobility for Inspection and Maintenance of 3D Complex Environments," *Autonomous Robots*, vol. 18, no. 2, pp. 157–169, 2005.
[30] K. Daltorio, A. Horchler, S. Gorb, R. Ritzmann, and R. Quinn, "A small wall-walking robot with compliant, adhesive feet," in *Proceedings of the IEEE/RSJ international conference on Intelligent robots and systems*, 2005.
[31] O. Unver, A. Uneri, A. Aydemir, and M. Sitti, "Geckobot: a gecko inspired climbing robot using elastomer adhesives," in *Robotics and Automation. Proceedings of IEEE International Conference on*, 2006, pp. 2329–2335.
[32] P. Menzel and F. D Aluisio, "BIOBOTS The movement to copy nature's critters in robotics labs around the world has produced some remarkably lifelike machines with extraordinary capabilities," *Discover-New York*, vol. 21, no. 9, pp. 86–93, 2000.
[33] M. Murphy and M. Sitti, "Waalbot: An agile small-scale wall-climbing robot utilizing dry elastomer adhesives," *Mechatronics, IEEE/ASME Transactions on*, vol. 12, no. 3, pp. 330–338, June 2007.
[34] M. Sitti and R. S. Fearing, "Synthetic gecko foot-hair micro/nano-structures as dry adhesives," *Journal of Adhesion Science and Technology*, vol. 17, no. 8, pp. 1055–1073, 2003.
[35] K. Autumn, C. Majidi, R. Groff, A. Dittmore, and R. Fearing, "Effective elastic modulus of isolated gecko setal arrays," *Journal of Experimental Biology*, vol. 209, no. 18, p. 3558, 2006.
[36] B. Aksak, M. P. Murphy, and M. Sitti, "Gecko inspired micro-fibrillar adhesives for wall climbing robots on micro/nanoscale rough surfaces," in *Robotics and Automation. IEEE International Conference on*, May 19-23 2008, pp. 3058–3063.
[37] S. Kim, M. Spenko, S. Trujillo, B. Heyneman, D. Santos, and M. R. Cutkosky, "Smooth vertical surface climbing with directional adhesion," *IEEE Transactions on Robotics*, vol. 24, no. 1, pp. 65–74, 2008.
[38] H. Prahlad, R. Pelrine, S. Stanford, J. Marlow, and R. Kornbluh, "Electroadhesive robotswall climbing robots enabled by a novel, robust, and electrically controllable adhesion technology," in *Robotics and Automation. Proceedings of IEEE International Conference on*, May 19-23 2008.
[39] A. Asbeck, S. Kim, W. Provancher, M. Lanzetta, and C. M.R., "Scaling hard vertical surfaces with compliant microspine arrays," *IJRR*, 2006.
[40] G. Wile, K. Daltorio, E. Diller, L. Palmer, S. Gorb, R. Ritzmann, and R. Quinn, "Screenbot: Walking inverted using distributed inward gripping," in *Intelligent Robots and Systems. IEEE/RSJ International Conference on*, 2008, pp. 1513–1518.
[41] K. Autumn, M. Buehler, M. Cutkosky, R. Fearing, R. J. Full, D. Goldman, R. Groff, W. Provancher, A. A. Rizzi, U. Saranli, A. Saunders, and D. E. Koditschek, "RiSE; robotics in scansorial environments," in *Proc. SPIE. 2005, Unmanned ground vehicle technology VII: 29-31 March*, 2005, pp. 291–302.
[42] A. Saunders, D. I. Goldman, R. J. Full, and M. Buehler, "The RiSE climbing robot: Body and leg design," in *Proceedings of SPIE - The International Society for Optical Engineering*, vol. 6230, 2006, p. 623017.
[43] J. Clark, D. Goldman, P.-C. Lin, G. Lynch, T. Chen, H. Komsuoglu, R. Full, and D. Koditschek, "Design of a bio-inspired dynamical vertical climbing robot," in *Proceedings of Robotics: Science and Systems*, June 27-30 2007.
[44] G. Lynch, J. Clark, and D. Koditschek, "A self-exciting controller for high-speed vertical running," in *Proceedings of the IEEE/RSJ international conference on Intelligent robots and systems*, 2009, pp. 631–638.
[45] L. P. Kalra, S. Weimin, and J. Gu, "A wall climbing robotic system for non destructive inspection of above ground tanks," in *Electrical and Computer Engineering, Canadian Conference on*, 2006, pp. 402–405.
[46] T. Bretl, S. Rock, and J. C. Latombe, "Motion planning for a three-limbed climbing robot in vertical natural terrain," in *Robotics and Automation. Proceedings of the IEEE International Conference on*, vol. 3, 2003, pp. 2946–2953.
[47] J. R. Usherwood and J. E. A. Bertram, "Understanding brachiation: insight from a collisional perspective." *The Journal of Experimental Biology*.
[48] J. Nakanishi, T. Fukuda, and D. E. Koditschek, "Preliminary studies of a second generation brachiation robot controller," in *Robotics and Automation. Proceedings of the IEEE International Conference on*, vol. 3, 1997, pp. 2050–2056.
[49] F. Saito, T. Fukuda, and F. Arai, "Swing and locomotion control for two-link brachiation robot," in *Robotics and Automation. Proceedings of the IEEE International Conference on*, vol. 2, 1993, pp. 719–724.
[50] S. A. Bailey, J. G. Cham, M. R. Cutkosky, and R. J. Full, "Comparing the locomotion dynamics of the cockroach and a shape deposition manufactured biomimetic hexapod," *Experimental Robotics*, vol. VII, pp. 239–248, 2001.
[51] J. Weingarten, G. Lopes, M. Buehler, R. Groff, and D. Koditschek, "Automated gait adaptation for legged robots," in *IEEE International Conference on Robotics and Automation*, vol. 3, 2004, pp. 2153–2158.
[52] S. Jensen-Segal, S. Virost, and W. R. Provancher, "ROCR: Dynamic vertical wall climbing with a pendular two-link mass-shifting robot," in *Proc. of the IEEE International Conference on Robotics and Automation*, May 19-23 2008, pp. 3040–3045.
[53] S. I. Jensen-Segal, "ROCR: Dynamically climbing sheer walls with a pendular two-link mass-shifting robot," Master's thesis, University of Utah, December 2009.
[54] R. Blevins, *Formulas for natural frequency and mode shape*. Van Nostrand Reinhold, 1979.
[55] K. Autumn, S. T. Hsieh, D. M. Dudek, J. Chen, C. Chitaphan, and R. J. Full, "Dynamics of geckos running vertically," *Journal of Experimental Biology*, vol. 209, no. 2, pp. 260–272, January 15 2006.
[56] P. Gregorio, M. Ahmadi, M. Buehler, S. Design, and Q. Montreal, "Design, control, and energetics of an electrically actuated leggedrobot," *IEEE Transactions on Systems, Man, and Cybernetics, Part B*, vol. 27, no. 4, pp. 626–634, 1997.

William R. Provancher has earned a B.S. in Mechanical Engineering and an M.S. in Materials Science and Engineering, both from the University of Michigan. His Ph.D. from the Dept. of Mechanical Engineering at Stanford University was in the area of haptics, tactile sensing and feed-back. His post-doctoral research involved the design of bioinspired climbing robots. He is currently an Assistant Professor in the Department of Mechanical Engineering at the University of Utah. He teaches courses in the areas of mechanical design, mechatronics, and haptics. His active areas of research include haptics and the design of novel climbing robots. Dr. Provancher received a Best Paper Award at the 2009 World Haptics Conference for his work on tactile feedback for the communication of direction. Details of his research and related publications are linked of off Dr. Provancher's homepage: http://www.mech.utah.edu/wil/

Samuel I. Jensen-Segal has earned a B.S. in Physics from Bates College and an M.S. in Mechanical Engineering from the University of Utah. His Masters thesis focused on developing the current prototype of ROCR that is reported in this article. He is currently a research and development engineer at Sky Research in Hanover, NH.

Mark A. Fehlberg has earned a B.S. in Mechanical Engineering from Virginia Tech and an M.A. in Managerial Economics from the University of Oklahoma. He achieved the rank of Captain in the U.S. Army serving as a Maintenance Management Officer in the Ordnance Corps. He then worked as a manager for KPMG and went on to found Initech Inc., a financial management and systems consulting small business. He is currently pursuing a Ph.D. in Mechanical Engineering at the University of Utah. His dissertation research is in the area of haptics.